Iranian Journal of Hydrogen & Fuel Cell 1(2018) 57-69

Iranian Journal of Hydrogen & Fuel Cell

IJHFC

Journal homepage://ijhfc.irost.ir

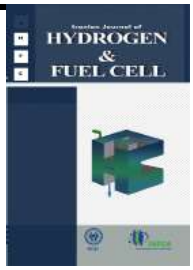

Buckypaper-based catalytic electrode containing graphene nanoplates and ZrO_2 nanorod composite to improve PEMFC performance

Maryam Yaldagard*

Department of Chemical Engineering, Urmia University, Iran

Article Information

Article History:

Received:
23 Sep 2018
Received in revised form:
20 Jan 2019
Accepted:
09 Feb 2019

Keywords

Buckypaper electrode
Nanofiber
Graphene nanoplates
ZrO_2 nanorods
PEMFC

Abstract

Many researchers have proposed the use of graphene nanoplates (GNPs), carbon nanofibers (CNFs), and metal oxide nanorods as an advanced metal catalyst support for electrocatalysis applications. In this research, a platinum (Pt) catalytic electrode was developed by using GNPs and CNFs containing ZrO_2 nanorods (buckypaper) as a supporting medium and the electrodeposition method to deposit Pt catalyst. Special mixed buckypapers (BPs) were developed by layered microstructures with a large porous structures of CNFs networks at the surfaceand dense and high-conducting GNP networks as back supports. This unique microstructure led to improved Pt catalyst accessibility and mass exchange properties. The topographical features, structure, morphology and composition of the prepared film samples were characterized by AFM, XRD, FESEM and EDX. The thickness of approximately 39 micrometer and a porosity of 81% were obtained by a porometer using the mercury prosimetry test. Catalytic properties of the Pt/BPs electrodes and MEA performance evaluations were measured using potensiostat/galvanostat and fuel cell test station based on cyclic voltammetry and single cell polarization measurements. Pt particles of about 6.66 nm were uniformly deposited in porous BPs. A promising electrochemical surface area of 31.66 m^2g^{-1} was obtained from these electrodes. The peak power density of the cell operated by BPs with ZrO_2 nanorods was 0.288 $kWcm^{-2}$, higher than 0.23 $kWcm^{-2}$ measured on the cell operated by the BPs without ZrO_2 nanorods. A Pt utilization as high as 0.675 $gPtkW^{-1}$ was achieved for the cathode electrode at 80°C. Pt utilization efficiency can be further improved by optimization of the electrodeposition condition in order to reduce the Pt particle size.

1. Introduction

Proton exchange membrane fuel cells (PEMFCs) are considered a promising power source for vehicles as well as portable and stationary applications because of their high efficiency, low emissions and quick

*Corresponding Author's Fax: +984432775660
E-mail address: m_yaldagard@yahoo.com

doi: 10.22104/ijhfc.2019.3158.1178

start-up. Since the first application of PEMFCs as a backup power source in the Gemini space flights in the 1960s, great efforts have been made towards commercializing PEMFCs to increase stack power density and membrane electrode assembly (MEA) performance. Among the various components that make up a MEA, the electrodes are a key factor in determining its catalytic performance. Improving the platinum (Pt) utilization contained in an electrode and optimize electrode structure simultaneously can lead to a substantial power density enhancement of the stack components. Generally, cathode and the anode electrodes are composed of a catalyst and support. In the state-of-the-art PEMFC, carbon black is usually used as the catalyst support material. The support material can considerably affect catalyst performance. The ideal support for a PEMFC electrocatalyst should have the following characteristics: large specific surface area with high mesoporous content, high electrical conductivity, good gas permeability, adequate water handling capability and good corrosion resistance, especially under highly oxidizing conditions occurring at the cathode. Some carbon blacks, such as Vulcan XC-72 R, meet most of these requirements. However, plentiful micropores in these carbon blacks can trap Pt nanoparticles, resulting in failure to establish three-phase boundaries among the gas, electrolytes and electrocatalysts. This fraction of Pt is therefore not utilized since the electrochemical reactions cannot occur at these sites, which will cause a reduction of Pt utilization. In addition, carbon black can be corroded under the severe conditions in the cathode, resulting in low cell stability and short service life. Recently, carbon nanofibers and graphene nanoplates have been explored as catalyst supports in PEMFC because of their unique properties, e.g. a high conductivity of about 100-10000 Scm^{-1} and large specific surface areas of up to 450 m^2g^{-1}, respectively[1].

Buckypapers, first proposed in 1998, are free-standing thin films consisting of single-walled carbon nanotubes (SWNTs), multi-walled carbon nanotubes (MWNTs), and/or carbon nanofibers held together by van der Waals forces without any chemical binders formed in a controlled manner[2]. Buckypapers are typically produced by a conventional filtration process where carbon nanotube (CNT) dispersed in aqueous medium were filtered through a membrane filter with the aid of vacuum, fabricating a random CNT bundles or ropes network on the membrane. This process can produce homogeneous mixing and reduce binder usage [3-5].

As an environmentally benign technology with wide applications, microwave synthesis has the advantages of homogeneous volumetric heating and a high reaction rate compared with other physical and chemical methods. In this study, we reported the synthesis of ZrO_2-nanorods arrays through the microwave method without any catalysts, templates, and substrates using zirconia chloride as zirconia source and strong aqua ammonia as both alkaline and complexing reactant. Furthermore, as an effective method for preparing cathode and anode electrodes, the buckypaper method was introduced. In this method ZrO_2 nanorods were uniformly dispersed and attached on the surface of conductive carbon nanofibers and high surface area Graphene nanoplates. A semi buckypaper electrode containing a ZrO_2/GNP/CNF composite is expected to show enhanced electrochemical performance due to its increased catalytic active area and improved electronic contact between the support and the catalyst.

2. Experimental

2.1. Materials

High-purity graphite powder (99.9999%, 200 mesh) was purchased from Alfa Aesar. Chemicals $H_2PtC_{16}.6H_2O$ (40%), hydrazine hydrate, $KMnO_4$ and H_2O_2, zirconia chloride and CNFs were obtained from Sigma-Aldrich. All solvents including H_2SO_4, 2-propanol, Tiritoon X100, aqua ammonia were used as received from Sigma–Aldrich without further purification. Nafion® solution (Ion power Inc,

Inc, USA 5 wt%), carbon cloth (Teflon treated), Nafion membrane 112, Teflon emulsion, carbon powder (Vulcan-XC-72R), and Pt/C(20wt%) were bought from the Fuel Cell earth company. High purified N_2 (99.9995%), O_2, and H_2 (99.99%) gases were purchased from Canadian Sigma Inc. Water purified by a Milli-Q water purification system was used throughout the electrodeposition experimental work.

2.2. Methods

2.2.1 Synthesis of ZrO_2-nanorods array

In a typical procedure, zirconia chloride was added into a 100 mL capacity glass beaker with 40 or 80 mL deionized water. The zirconia chloride (1 or 2 mmol) was dissolved assisted by ultrasound equipment. Then ammonia solution (30%) was added dropwise to the above solution with constant stirring. After stirring at room temperature for 5min, the above samples were irradiated by microwave energy using the commercial microwave digestion system (model: WX-4000, Microwave digestion system) with an irradiation time of 3 min and work power of 1000W. After microwave processing, the solution of the mixture was cooled to room temperature naturally. The resulting precipitates were collected by filtration and washed with deionized water for several minutes. The final products were dried in a vacuum oven at 60 °C for 2 h [6].

2.2.2. Chemical Preparation of Graphene Oxide (GO) and GNPs

In a typical synthesis process, natural graphite powder was oxidized to graphite oxide by a modification of Hummers and Offenman's method [7]. In brief, 2 g graphite powder and 1g sodium nitrate were transferred into 90 ml concentrated H_2SO_4 in ice bath conditions. Then 6g $KMnO_4$ was regularly added. The mixture was stirred at 35±5°C for 8 h. Then, deionized water (DI) with a volume of 200 ml was added and then diluted with 400 ml DI. After that 5% H_2O_2 was added into the solution until the colour of the mixture altered from brown to peril yellow. The solution was filtrated via vacuum buchner filtration and the filter cake dispersed in DI by means of an ultrasonic bath. The mixture was washed with 1:20 HCL solution and water by repeated centrifugation which operated in 11000 rpm for 20 min to pH value of 7 and then dried in vacuum oven at 60°C for 24 h. The as obtained graphite oxide was dispersed in DI water and exfoliated to generate graphene oxide by ultrasonication using a sonifier (UP400 S, 80 amplitue). The brown graphene oxide nanoplates dispersion was transferred into a round-bottomed flask, to which hydrazine monohydrate (as reducing agent) was added. The mixed solution was then refluxed at 100 °C for 2 h, over which the colour of the solution gradually changed to dark black as the graphene nanosheets dispersion floating at the air/solution interface of the dispersion was formed. The dispersion was further centrifuged for 15 min at 3000 rpm to remove a small amount of precipitate. The supernatant of the graphene nanosheets dispersion was directly dried in a vacuum oven to obtain the bulk of graphene nanosheet powders.

2.2.3. Prepration of bucky paper

ZrO_2 nanorods-GNP-CNF mixed buckypaper sheets were produced using a vacuum filtration method. A mixture of GNPs and CNFs (w/w, 1:3) and ZrO_2 nanorods in 1000 mL deionized water was sonicated to achieve a homogenous dispersion by adding Triton-X as a surfactant. The suspension was then filtered under a vacuum through a nylon membrane (Millipore, 0.45 m in pore size). The sediment was washed thoroughly with isopropanol to remove the residual surfactant. After drying, a thin film layer was peeled from the filter membrane to produce a free-standing buckypapers (BPs).

2.2.4. Electrodepositions of Pt Nanoparticles

The mixed buckypapers were washed with isopropanol to remove the most of surfactant before preparing Pt/

BP electrodes. For the synthesis of BP-supported Pt catalysts, several catalyst synthesis methods, such as impregnation method, sonochemical technique, microwave heated polyol process, electrodeposition, sputter-deposition technique, and others have been mentioned in the literatures. However, the first three techniques severely destroy buckypapers under stirring in solutions. In this research, we adopt the electrodeposition method for Pt deposition on the buckypapers surface. Using the tube furnace, the surfactant of buckypapers was further burned out in nitrogen at 400 °C for two hours for all samples.

In the electrodepostion method, a traditional three-electrode cell setup was saturated with calomel electrode (SCE) as the reference electrode and platinum foil as the counter electrode. The working electrode was a piece of as prepared buckypapers which was loaded on a home-made sample holder coupled with a hydrophobic carbon cloth as a current collector. The electrodeposited size of the buckypapers was 5 cm² lain on the window size of the sample holder exposed to the electrolyte. The platinum was electrochemically deposited on buckypapers by a galvanic pulse current in a solution of 10 mM H_2PtC_{l6}, 0.1 M H_2SO_4, and 0.5M ethylene glycol (EG) with N_2 bubbling. The peak current density was 300 $mAcm^{-2}$ and on/off time of 10/100 ms with duty cycle of 10% for the electrode of interest. The amount of Pt loading was determined by weighing the mass increase after deposition (by initial BPs weight and weight of the sample after Pt electrodepositon on BPs afterwards the drying). For comparison purposes, Pt nanoparticles with the same content were electrodeposited on the surface of GNP/CNF buckypapers without the ZrO_2 nanorods.

2.3. Fabrication of MEA

The electrochemical implement of the Pt/BP electrocatalysts as a cathode catalyst layer was determined in a single 5 cm² PEMFC. The anode catalyst was commercial 20 wt% Pt/C, and the membrane was Nafion-112 (Dupont) pretreated with H_2O_2 and H_2SO_4. For both cathode and anode catalyst electrodes, a two-layer structure was used as the gas diffusion layer (GDL): the outer layer was teflonized (30 wt% Teflon in cathode, 10 wt% in anode) carbon cloth and the inter layer (between the carbon cloth and catalyst layer) was prepared by spraying an isopropanol mixture of the Vulcan XC-72 carbon black and a 30 or 10 wt% Teflon emulsion onto the carbon cloth, which was then sintered at 340 °C for 1 h. For the anode, a Pt/C catalyst was applied using a conventional ink process. The proper amount of the Pt/C catalyst was mixed with 10 wt% Nafion in isopropanol and then sprayed on the inter GDL by a spray gun to constitute the catalyst layer with a Pt loading of 0.4 mg cm^{-2}. The Pt deposited buckypapers were placed on the cathode GDL to serve as a catalyst layer where the selected side of the buckypapers was exposed. Finally, a thin layer of Nafion solution (1.0 mg cm^{-2}) was spread onto the surface of each catalyst layer.

The membrane electrode assembly was formed by sandwiching the electrolyte membrane between the anode and cathode and hot pressing it at 125 °C for 60 s under 75 bar of pressure. The single cell was operated by a fuel cell testing system with humidified H_2 (30 ml min^{-1}, stoichiometric ratio of 1.5) as the fuel and humidified O_2 (20 ml min^{-1}, stoichiometric ratio of 2) as the oxidant. The operation conditions were: humidifier temperatureof 80 °C for both reactants, cell temperature of 80 °C, and gas pressure at 1.5 bar on both sides. The cell performance was recorded by electronic load assembled in the testing system.

2.5. Physical characterization and electrochemical measurements

X-ray powder diffraction (XRD) was carried out at room temperature with an Equinox 3000 (IENL France) using Cu Kα (λ=0.15406 nm) radiation generated at 40 Kv and 30 mA with resolutions of ≤0. 1 °. The 2θ angular between 10 ° and 90 ° were explored at a scan rate of 10 ° min^{-1}.

The particle morphology and size of Pt nanoparticles dispersed on the surface of buckypapers were characterized by Field emission–scanning electron

microscopy (FE-SEM) characterization and Energy dispersive X-ray (EDX) spectroscopy coupled to a scanning electron microscopy SEM MAG100.00 kx with a silicon detector performed at 15 kV.

The topography and further structure studying of the graphene sheets and ZrO_2 nanorods were examined by an Atomic Force Microscope (AFM, model Nanosurf easy scan2) using contact mode. The pore size distribution and gas permeability were determined using the homemade capillary flow porometer. Electrochemical measurements were conducted at conventional three-electrode cell using potensiostat/galvanostat model iviumstat–XRi electrochemical Interface System. Pt foil was served as a counter electrode while KCl saturated Ag/AgCl was used as a reference electrode. Electrode and MEA performance (I-V curve) in a single cell was performed in fuel cell testing system (Hefa Station, Fuel Cell Technologies).

3. Results and Discussion

3.1. Physical characterization

3.1.1. Properties of buckypapers

The as-produced ZrO_2 nanorods-GNP-CNF mixture buckypapers were approximately 39 micro meter thick with a porosity of 81%, which was measured by the mercury porosimetry method based on the gradual injection of liquefied Hg into the pore system with external pressure. Experimentally, about 0.96 cm^2 BPs specimens was placed in the porometer chamber to undergo low and high pressure mercury intrusion testing. Mercury was then forced to intrude into the voids in a porous BPs sample by increasing the pressure up to150 MPa, whereby the BPs sample pores were filled starting from the larger pores at low pressures to smaller and smaller pores at higher pressures. This method allowed the measurements and determination of total pore volume as well as total porosity values. The gas permeability of the BPs was characterized by measuring the time dependence of the pressure drop in a gas reservoir from which air was evacuated only through the buckypapers membrane. The rate of pressure deterioration was expected to be proportional to the pressure as in the well-known 1D gaseous diffusion problem. As shown in Fig. 1, the pressure (P) in the reservoir as a function of time (t) fitted the first order decay as given in Eq. (1) very well [5, 8].

$$P(t) = Const + P_0 e^{\frac{-t}{\tau}} \quad (1)$$

where P_0 is the initial pressure in the reservoir and the time constant can be described as:

$$\tau = \frac{V_u . l}{A.R.T.D_{eff}} \quad (2)$$

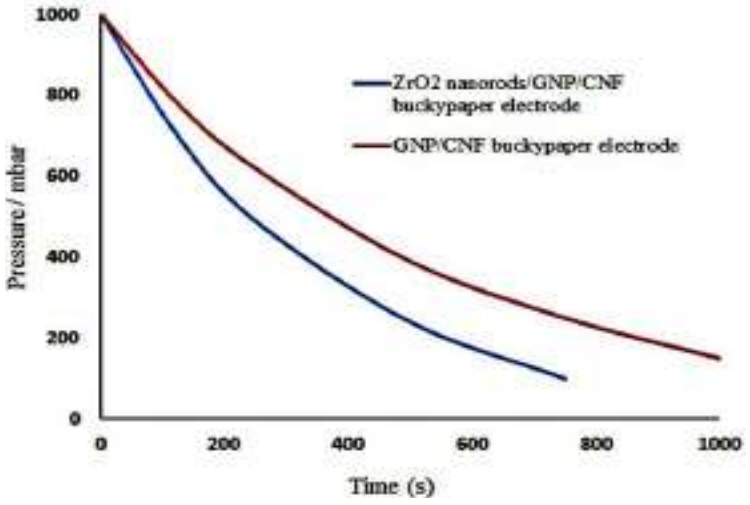

Fig. 1. pressure in the reservoir as a function of time by evacuating air through the buckypapers.

where V_u is the volume of the reservoir; l and A are the thickness and cross-section area of the buckypaper, respectively; R is the gas constant, and T is the temperature in the unit of K. The effective diffusivities (Deff) are accordingly calculated as 1.76 × 10^{-9} $molPa^{-1}m^{-1}s^{-1}$ for ZrO_2 nanorods-GNP-CNF and 1.14 × 10^{-9} $molPa^{-1}m^{-1}s^{-1}$ for GNP-CNF without ZrO_2 nanorods. GNP-CNF mixture buckypaper with ZrO_2 nanorods content has a larger pore size and porosity resulting in a higher permeability, which facilitates the mass transfer in the fuel cell.

3.1.2. XRD pattern characterization

Fig. 2 shows the X-ray diffraction patterns of the Pt/ZrO_2 nanorods-GNP-CNF electrode which reveal the diffraction peaks of both carbon and platinum. The sharper and narrow diffraction peaks at 2θ=26.518 ° (002) and 54.42 ° (004) are the characteristics of the parallel graphene layers and C in CNFs in Pt / ZrO_2 nanorods-GNP-CNF electrode which indicate a highly graphitic and crystallinity ordered structure of GNP in planes of (002) and (004), respectively. The peaks at the Bragg angles of 40.055 °, 46.60 °, 67.96 °, 81.78 °, and 86.38 ° corresponds to the (111), (200), (220), (311), and (222) crystalline plane diffraction peaks, respectively. All peaks can be indexed as the Pt face centered cubic (fcc) phase. In addition to the main characteristic peaks of the graphite and Pt fcc structure, several other reflections at 2θ=29.44 ° and 31.81° were found in the electrode which are related to a ZrO_2 nanorods array used in buckypaper composite. The average size of Pt particles (6.66 nm) were calculated from the Debby-Scherrer equation using the full width at half maximum (fwhm) of the (111) reflection. Pt (111) plane was selected for Scherrer analysis because it has the highest intensity value. This equation can be expressed as below [9]:

$$d = 0.9\frac{\lambda}{B\cos\theta} \quad (3)$$

Where d is the diameter of the average particle size in Å; λ is the X-ray wavelength (1.5406 Å) for CuK_α; θ is the Bragg angle, and B is the full width at half maximum (fwhm) in radians.

3.1.3. Topography and Structural Characterization of GNPs and ZrO_2 nanoroads

The obtained graphene nanoplates and nanorods array of ZrO_2 were analyzed by Atomic Force microscopy (AFM) to determine its thickness and lateral size, length, and diameter, respectively. Fig. 3 a, b and ,c show an AFM image of graphene nanoplates along with

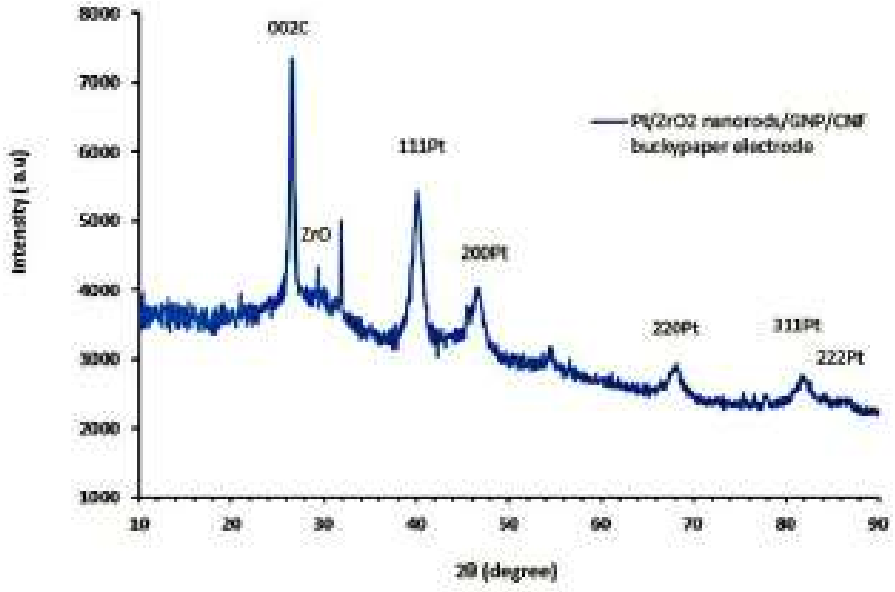

Fig. 2. X-ray diffractograms of the in Pt / ZrO_2 nanorods/GNP/CNF electrode.

corresponding height profile produced by chemical reduction from the exflotied graphene oxide, ZrO_2 nanorods arrays produced by microwave irradiation synthesistechniqueandaspreparedbuckypaperselectrode, respectively. The topographic height of the graphene nanoplates indicate a few-layered graphene nanoplates. The average length and diameter of ZrO_2 nanorods were about 1.5 micrometer and 44nm, respectively.

3.1.4. Morphology of ZrO_2 nanorods, buckypaper and Pt nanoparticles

The microstructures of the specimens have been investigated by FESEM. The results are presented in Fig. 4 (a-h) respectively. Well-dispersed Pt nanoparticles were observed on the buckypapers (Fig. 4 e, g, and h) with an average diameter of about 6nm. Fig. 4 c, d, and f shows the typical SEM images of the products prepared using 1.0 mmol $ZrCl_2$ and 5.0 mL NH_3H_2O solution at a power of 30% for 20 min. The image clearly reveals that the bulk-shaped structures are composed of nanorods. The nanorods lined up with each other are about 1-2 micrometer in length and 0.044 micrometer in diameter, though only a few flowers can be found. Fig. 4 (a, b) show the SEM images of raw CNF and prepared GO nanoplates, respectively. The images show that the large CNFs entangle to form a backbone where a fine meshwork

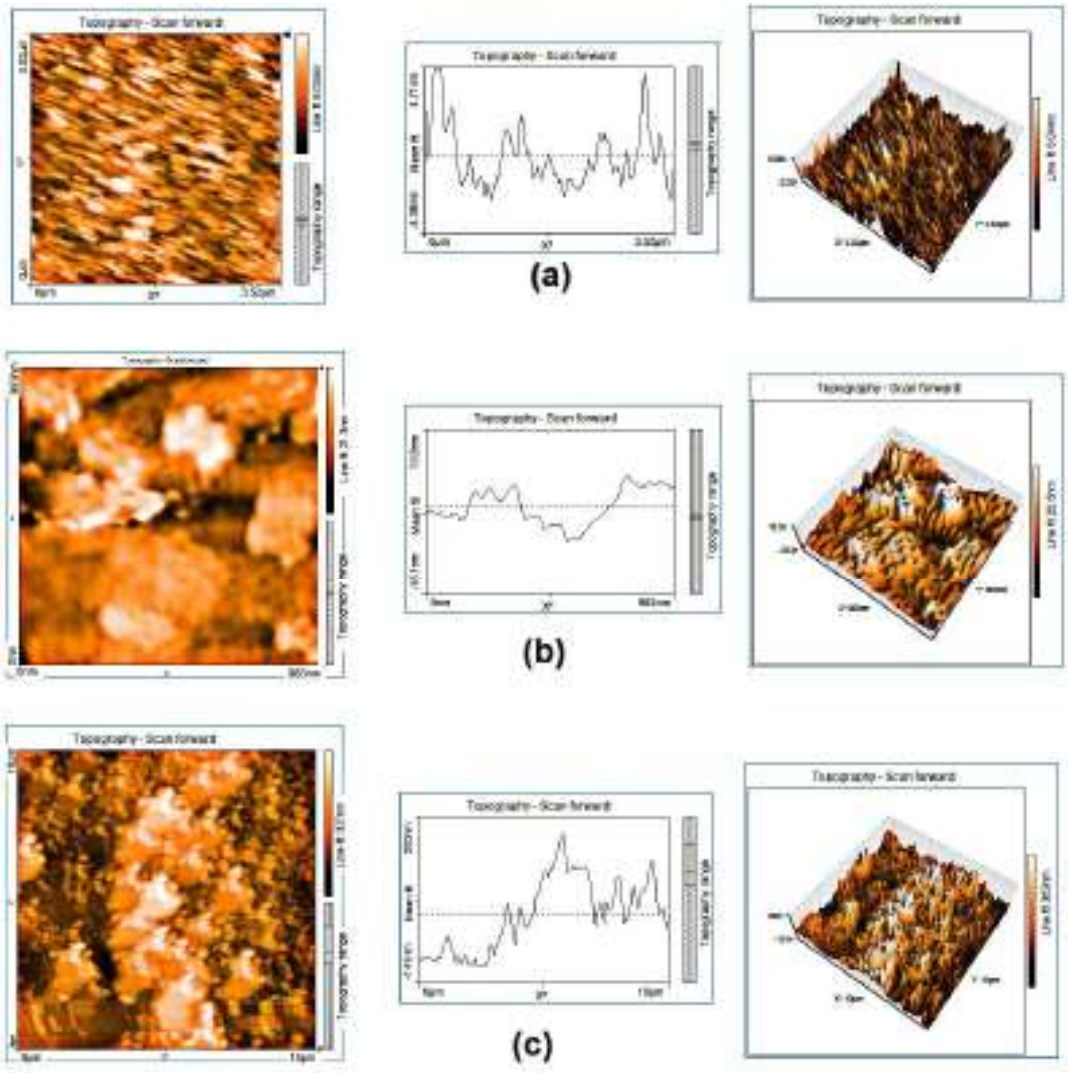

Fig.3. AFM topography images of a) nanorod arrays of ZrO_2, b) chemical reduced graphene nanoplates, c) prepared buckypaper. Next to the images are a line scan taken horizontally through the image as marked with an arrow, from which the height of a graphene nanoplates were determined.

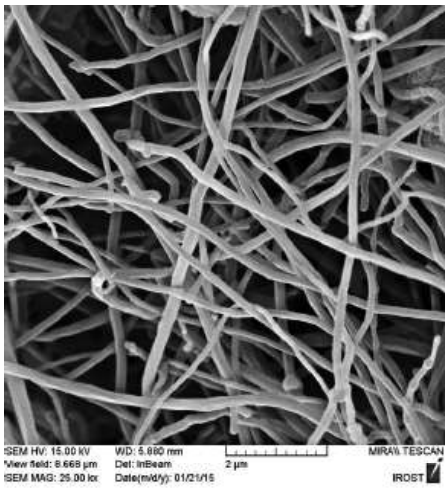

(a)

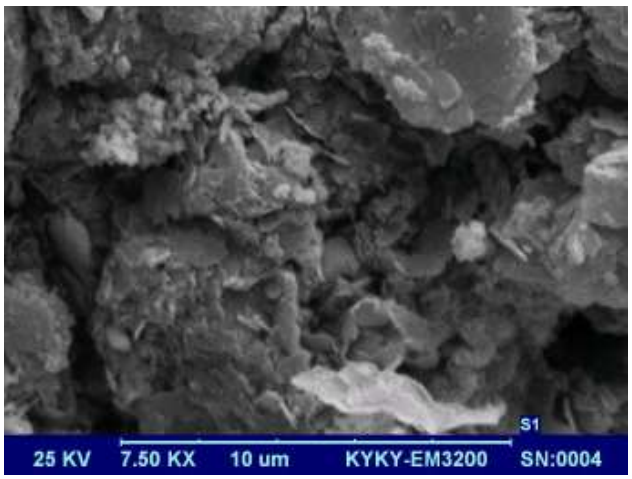

(b)

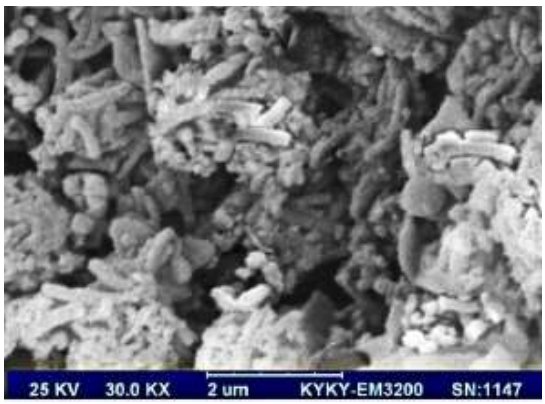

(c)

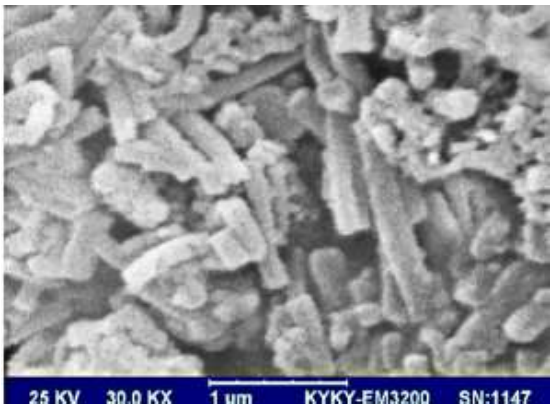

(d)

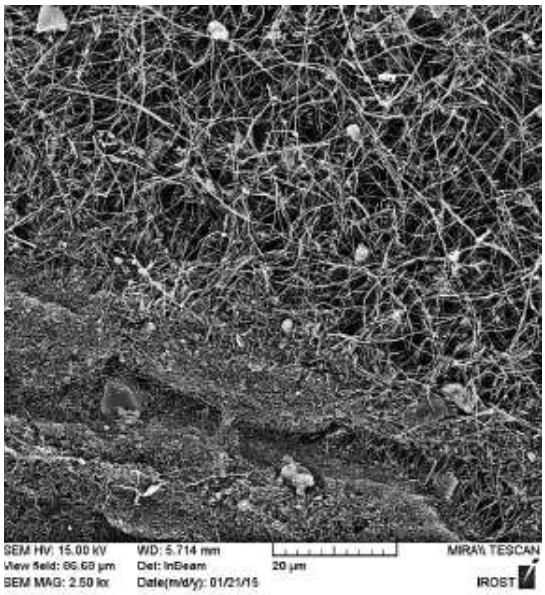

(e)

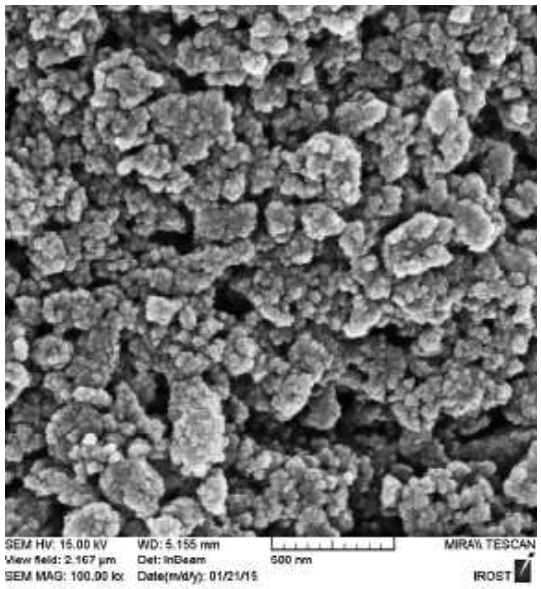

(f)

Fig.4. FESEM images of the a) CNF, b) graphene nanoplates, c,d,f) ZrO_2 nanorods, e,g,h) Pt/ZrO_2 nanorods/GNP/CNF electrode

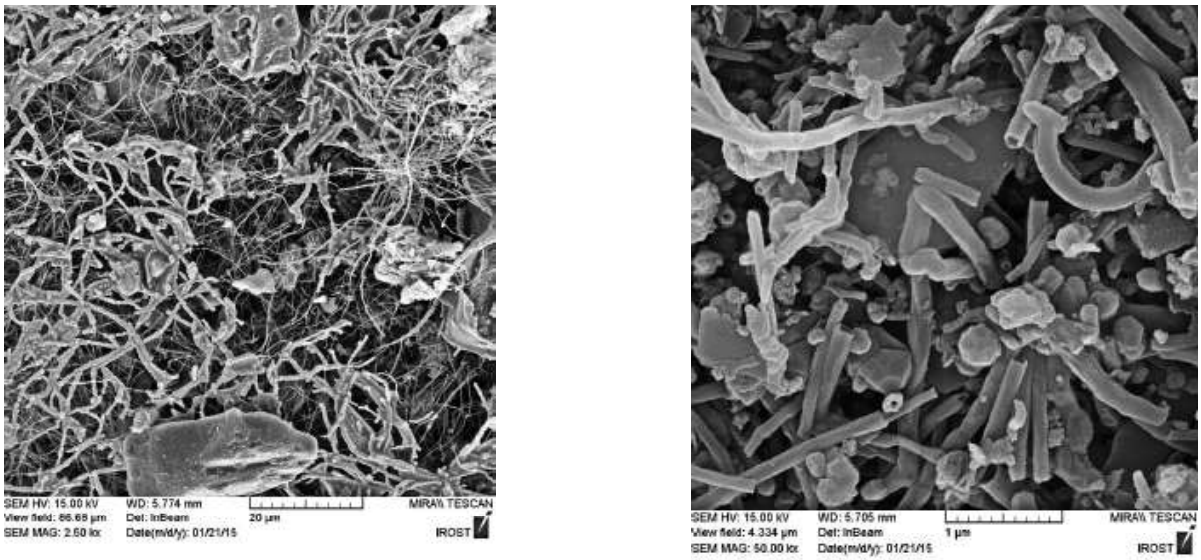

(g) **(h)**

Fig.4. FESEM images of the a) CNF, b) graphene nanoplates, c,d,f) ZrO_2 nanorods, e,g,h) Pt/ZrO_2 nanorods/GNP/CNF electrode (continued)

of much smaller GNPs creates the surface covering layer.

The EDS spectrum of Pt/ZrO_2 nanorods-GNP-CNF electrode is shown in Fig. 5. The EDS pattern shows that Pt, Zr, O and C are the major elements of spectra. The C signal comes from the graphene nanoplates and CNFs. Zr derived from ZrO_2 nanorods and oxygen is from the ZrO_2 and nafion solution. A small part of the oxygen may originate from an incomplete reduction from graphenen oxide to graphene. Besides Pt, Zr, O, and C, the elements of Si, Cl, Au, and S were detected as well. The strong peak of Si is because of the silicon substrate used in the FESEM analysis. Relatively small amount of S observed in the EDS image is essentially from the Nafion solution. The elements of Cl and Au belongs to the PtC_{l6} from the plating cell on the buckypaper and Au target is from the sputtering chamber in the FESEM chracterization, respectively.

3.2. Electrochemical and performance measurements

3.2.1. ECSA measurements

Fig. 6 shows the corresponding CV for the evaluation of the electrochemical reaction areas. For cyclic voltammetry measurements, the working electrode was immersed in a 0.5M H_2SO_4 solution saturated with high purified nitrogen gas (99.9995%) with the potential scan between -0.24V and 1.2 V versus Ag/AgCl at a scan rate of 50 mVs^{-1}. The cathodic and anodic peaks that appeared in the range from 0.05 to 0.4 V are considered because they are related to the adsorption and desorption reactions of hydrogen on the catalyst surface. The Pt electrochemical surface area (ECSA) were determined by measuring the area under the hydrogen adsorption/desorption peaks of the CV curves in 0.5 M H_2SO_4: [10].

$$ECSA = \frac{Q}{[Pt] \times 0.21} \quad (4)$$

Where [Pt]: the platinum loading ($mgcm^{-2}$) in the electrode

Q: the charge for hydrogen adsorption ($mCcm^{-2}$)

0.21: the charge required to oxidize a monolayer of H_2 on bright Pt

According to Fig. 7, the ECSA is larger in the Pt/buckypapers containing ZrO_2 nanaorods than Pt/buckypapers without ZrO_2 (31.66 vs 14.28 m^2g^{-1}). This indicates that a greater amount of active sites might be offered in the hydrogen adsorption and desorption reactions. As a result, a greater proportion of Pt

is utilized in the buckypapers containing a ZrO_2 nanaorods catalyst layer; therefore, it shhould have more efficient electrocatalyst reactions and better performance of PEMFC.

3.2.2. Electrochemical Impedance Spectroscopy (EIS) Studies of the Electrodes

The half cell polarization studies, a powerful technique to study the interface process of electrodes, were complemented with EIS analysis for an in-depth investigation into the two electode's behavior. In these measurements, the buckypaper electrodes were exposed to an O_2 saturated aqueous solution of 0.5M H_2SO_4. An alternating sinusoidal signal of 5mV peak to peak was superimposed on the d.c potential. The impedance spectrum was collected by sweeping frequencies over the range of 1 mHz to 100 KHz with 55 points/decade. The corresponding Nyquist plots are shown in Fig. 7. As can be seen, both of the impedance spectra display similar characteristics, i.e., a depressed arc in the high frequency region,

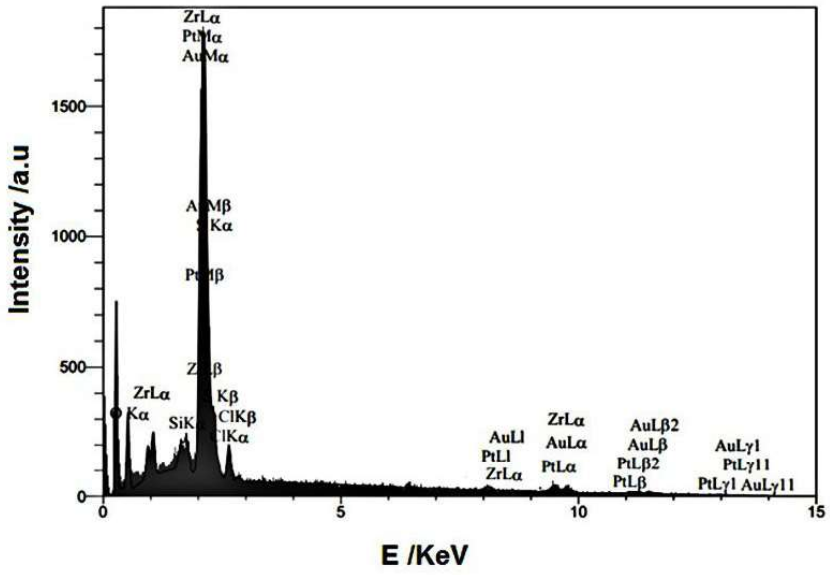

Fig.5. EDX pattern of Pt / ZrO_2 nanorods/GNP/CNF electrode.

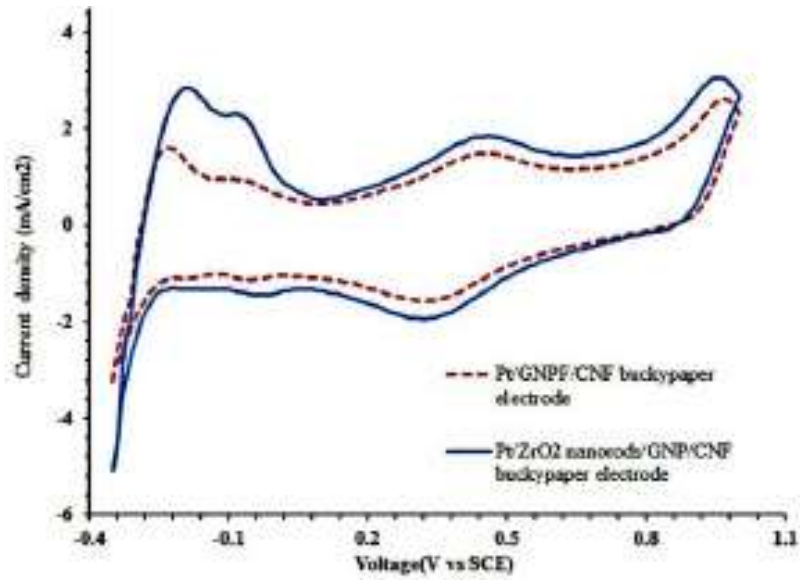

Fig.6. Cyclic voltamograms of methanol oxidation of Pt / ZrO_2 nanorods-GNP-CNF buckypaper electrode and Pt / GNP-CNF buckypapers electrode in 0.5M H_2SO_4 solution scan rate: 50 mV s^{-1}.

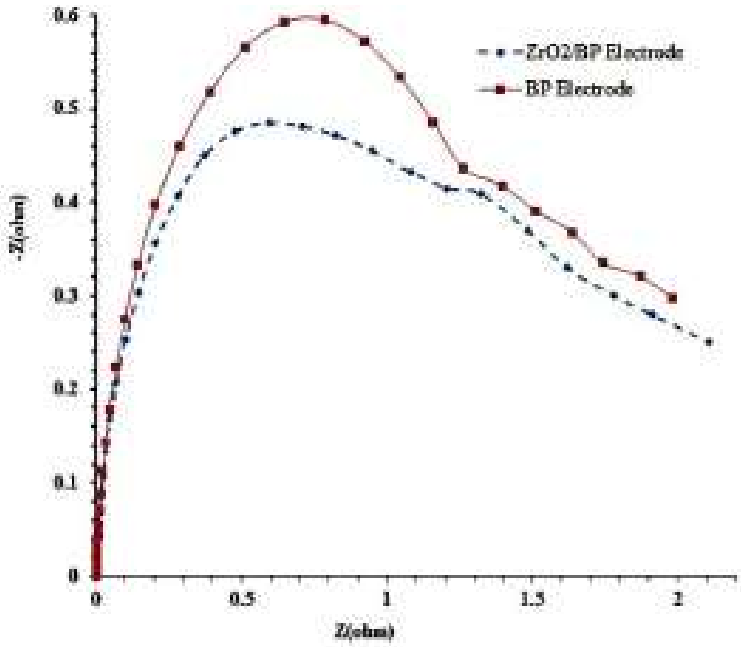

Fig.7. Impedance response in the Nyquist form of the Pt /ZrO_2 nanorods-GNP-CNF buckypaper electrode and Pt / GNP-CNF buckypaper electrode in 0.5M H_2SO_4 at 25C under O_2 flux.

whose diameters is associated with the charge transfer resistance indicating catalytic activity for ORR and an additional arc in the low frequency region which corresponds to diffusion-limited of the support. From the fact that diffusion-limited strongly depends on the GDL characteristics like thickness, etc. it is hypothesized that the low-frequency arc in their impedance data is caused by oxygen diffusion through the byckypaper which is in good agreement with previous results [11]. In this plot, as it is clearly seen that the diameter of the arc in Pt/ZrO_2 nanorods-GNP-CNF buckypapers electrode is small in comparison with the impedance spectra of Pt/GNP-CNF buckypapers electrode without ZrO_2 nanorod. In the other words, the charge transfer resistance of the Pt/ZrO_2 nanorods-GNP-CNF buckypapers electrode is much lower than that of Pt/GNP-CNF buckypapers electrode showing the high activity for ORR.

3.2.3. Electrode performance in a single cell

Current density-voltage and current-power density curves (single cell performance) for the cell using the buckypapers with ZrO_2 nanorod (cell I) and the buckypapers without ZrO_2 nanorods (cell II) as the cathode based MEA with a Pt loading of 0. 4 $mgcm^{-2}$ are presented in Fig. 8. The cell outputs achieved at 80 °C with a back pressure of 20 psi were 430 $mAcm^{-2}$ for cell I and 330 $mAcm^{-2}$ for cell II both at 0.65 V. The peak power density of the cell worked by buckypapers with ZrO_2 nanorods was 0.288 $kWcm^{-2}$, higher than the 0.23 $kWcm^{-2}$ measured on the cell worked by the buckypapers without ZrO_2 nanorods. The Pt utilization in MEA, defined as the Pt loading divided by the cell output power at 0.65 V, was 0.67 gPt kW^{-1} for the buckypapers with ZrO_2 nanorods cathode and 0.5 gPt kW^{-1} for the buckypapers without ZrO_2 nanorods cathode. The higher Pt utilization achieved by Pt /ZrO_2 nanorods-GNP-CNF electrode catalyst may be due to the fact that the larger pore size and porosity and higher permeability introduced by ZrO_2 nanorods, facilitate the mass transfer in the catalyst layer. It is also believed that the Pt utilization of the Pt/ ZrO_2 nanorods/buckypapers electrode can be further improved to larger than 0.67 gPt kW^{-1}, which can fulfill the future requirements of PEMFC electrocatalysts for automotive application [12] by reducing the Pt particle size to 2–3 nm.

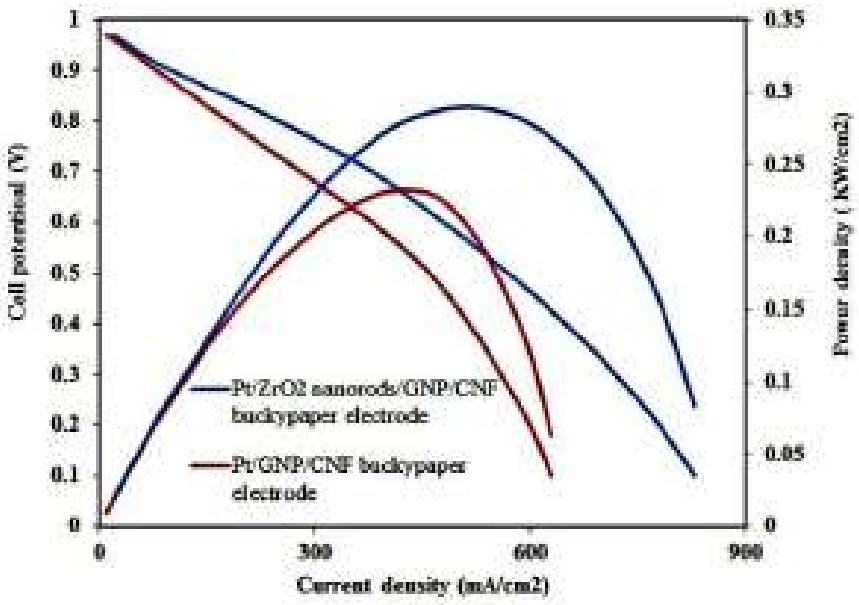

Fig.8. Cell polarization curves: Current density-voltage, current density-power density.

4. Conclusion

In this article a novel ZrO_2 nanorods-GNP-CNF hybrid material was prepared via the buckypaper method and demonstrated promise for cathode electrode in fuel cell application. The cyclic voltammetry and Current density-voltage/Current density-power density curves for the cathode electrode /MEA containing ZrO_2 nanorods results exhibited an improved electrochemical surface area and single cell performance better than that of the cathode electrode/ MEA fabricated by buckypapers without ZrO_2 nanorods under identical test conditions. The peak power density of the cell worked by buckypapers with ZrO_2 nanorods was 0.288 $kWcm^{-2}$, higher than 0.23 $kWcm^{-2}$ measured on the cell worked by the buckypapers without ZrO_2 nanorods. In other words, the MEA produced by buckypaper with ZrO_2 nanorod illustrated better catalyst utilization, higher ESA, more intimate membrane/electrode interface, and greater number of triple phase boundary sites than that produced by the buckypapers without ZrO_2 nanorods.

References

[1] Antolini, E., "Carbon supports for low-temperature fuel cell catalysts", Appl. Catal. B: Environ., 2009,88: 1.

[2] Rinzler, A., Liu, J., Dai, H., Nikolaev, P., Huffman, C., Rodriguez-Macias, F., Boul, P., Lu, A.H., Heymann, D.andColbert, D., "Large-scale purification of single-wall carbon nanotubes: process, product, and characterization", Appl. Phys. A: Mater. Sci. & Processing, 1998,67: 29.

[3] Kim, D.S.andPark, Y.J., "Buckypaper electrode containing carbon nanofiber/Co_3O_4 composite for enhanced lithium air batteries", Solid State Ionics, 2014,268: 216.

[4] Brown, B., Swain, B., Hiltwine, J., Brooks, D.B.andZhou, Z., "Carbon nanosheet buckypaper: A graphene-carbon nanotube hybrid material for enhanced supercapacitor performance", J. Power Sources, 2014,272: 979.

[5] Zhu, W., Ku, D., Zheng, J., Liang, Z., Wang, B., Zhang, C., Walsh, S., Au, G.andPlichta, E., "Buckypaper-based catalytic electrodes for improving platinum utilization and PEMFC's performance", Electrochim. Acta, 2010,55: 2555.

[6] Zhu, J.-Y., Zhang, J.-X., Zhou, H.-F., Qin, W.-Q., Chai, L.-Y.andHu, Y.-H., "Microwave-assisted synthesis and characterization of ZnO-nanorod arrays", T. Nonferr.

Metal. Soc, 2009,19: 1578.

[7] Wang, G., Shen, X., Wang, B., Yao, J.andPark, J., "Synthesis and characterisation of hydrophilic and organophilic graphene nanosheets", Carbon, 2009,47: 1359.

[8] Smajda, R., Kukovecz, Á., Kónya, Z.andKiricsi, I., "Structure and gas permeability of multi-wall carbon nanotube buckypapers", Carbon, 2007,45: 1176.

[9] Culity, B.andStock, S., "Elements of X-ray Diffraction", Edison Wesley, London, 1978, pp. 99.

[10] Pozio, A., De Francesco, M., Cemmi, A., Cardellini, F.andGiorgi, L., "Comparison of high surface Pt/C catalysts by cyclic voltammetry", J. power sources, 2002,105: 13.

[11] Ciureanu, M.andRoberge, R., "Electrochemical impedance study of PEM fuel cells. Experimental diagnostics and modeling of air cathodes", J. Phys. Chem. B, 2001,105: 3531.

[12] Gasteiger, H.A., Kocha, S.S., Sompalli, B.andWagner, F.T., "Activity benchmarks and requirements for Pt, Pt-alloy, and non-Pt oxygen reduction catalysts for PEMFCs", Appl. Catal. B: Environ., 2005,56: 9.